

Room-Temperature Vibrational Difference Spectrum for $S_2Q_B^-/S_1Q_B$ of Photosystem II Determined by Time-Resolved Fourier Transform Infrared Spectroscopy

Haoming Zhang,^{*,‡,||} Gad Fischer,[§] and Tom Wydrzynski^{*,‡}

Research School of Biological Sciences, Institute of Advanced Studies and Department of Chemistry, Faculty of Science,
The Australian National University, Canberra, ACT 0200, Australia

Received July 22, 1997; Revised Manuscript Received February 11, 1998

ABSTRACT: Time-resolved FTIR spectroscopy has been used to kinetically characterize the vibrational properties of intact photosystem II-enriched membrane samples undergoing the S_1Q_B -to- $S_2Q_B^-$ transition at room temperature. To optimize the experimental conditions for the FTIR measurements, oxygen polarographic and variable chlorophyll *a* fluorescence measurements were used to define the decay of S_2 and Q_A^- , respectively. The flash-induced $S_2Q_B^-/S_1Q_B$ difference spectra were measured at a temporal resolution of 4.44 s and a spectral resolution of 4 cm^{-1} . An intense positive band is observed at 1480 cm^{-1} in the difference spectrum and shows a slow decay with a half time of ~ 13 s. Based on its decay kinetics and analogy to the infrared absorption of Q_A^- of photosystem II and Q_B^- in bacterial reaction centers, we conclude that the 1480 cm^{-1} band arises from Q_B^- of PSII and tentatively assign it to the $\nu(\text{CO})$ mode of the semiquinone anion Q_B^- . The infrared spectral features attributed to the S_1 -to- S_2 transition of the Mn cluster at room temperature show striking similarity to the S_2/S_1 difference spectrum measured at cryogenic temperatures (Noguchi, T., Ono, T.-A., and Inoue, Y. (1995) *Biochim. Biophys. Acta* 1228, 189–200).

Photosynthetic water oxidation occurs in photosystem II (PSII),¹ where the light energy absorbed by the light-harvesting pigment molecules is transferred into the reaction center (RC) and induces a charge separation to occur between the primary chlorophyll donor molecule P_{680} and a pheophytin acceptor molecule, forming the $P_{680}^+\text{Phe}^-$ radical pair within a few picoseconds (*1*). To stabilize the charge separation, the electron is further transferred to the primary plastoquinone (PQ) acceptor Q_A and then to the secondary plastoquinone acceptor Q_B molecule. Q_A acts as a one-electron intermediate and is tightly bound, while Q_B acts as a two-electron gate. Singly reduced Q_B is tightly bound as a semiquinone anion, Q_B^- , while the doubly reduced Q_B is released as plastoquinol, PQH_2 , and replaced by another plastoquinone molecule from the PQ pool. On the donor side of PSII the oxidizing equivalents are accumulated, via the redox-active tyrosine residue Y_Z , on the O_2 evolving complex (OEC) which contains a cluster of four Mn ions. The OEC cycles through five intermediate redox states termed S_i (where $i = 0-4$). Upon reaching the S_4 state, O_2

is released and the cycle begins again. The S_0 and S_1 states are dark stable (for reviews, see refs 2–4).

To probe for the protein ligation and structural changes associated with the photoreduction of the plastoquinones and the photooxidation of the S-states, Fourier transform infrared (FTIR) spectroscopy has been used. The S_2/S_1 difference spectrum was first characterized by Noguchi et al. (5) in trypsin-treated PSII samples at 250 K in the presence of 20 mM ferricyanide following a single flash excitation. Mild trypsin treatment was used to modify the Q_B site in order to enhance electron flow from Q_A^- to ferricyanide without affecting the donor side. Under these conditions, contributions from the acceptor side of PSII were minimized. In a later work (6), the infrared S_2/S_1 difference spectrum was obtained in untreated PSII at 250 K in the presence of 2 mM/18 mM ferri/ferrocyanide at pH 5.5. On the basis of a temperature-dependent study of the $S_2Q_A^-/S_1Q_A$ difference spectrum (80 K – 240 K), Noguchi et al. (7) identified a negative band at 1404 cm^{-1} as characteristic of the S_1 -to- S_2 transition and suggested that this band arises from the symmetric vibration of a carboxylate group which ligates to the Mn cluster. By comparison of the difference spectra obtained at 140 and 200 K where the EPR $g = 4.1$ and multiline signals from the Mn cluster are generated, respectively, it was proposed that there is no significant structural change in the Mn cluster in these two states. More recently, the $S_2Q_A^-/S_1Q_A$ difference spectrum has been investigated under conditions which are believed to optimize separately the formation of the multiline and $g = 4.1$ signals in a glycerol-containing medium (8). By contrast, in this work

* Authors to whom correspondence should be addressed.

‡ Research School of Biological Sciences.

§ Department of Chemistry.

|| Present address: Department of Chemistry and Biology, University of Québec at Trois-Rivières, Québec, Canada G9A 5H7

¹ Abbreviations: DCMU, 3-(3,4-dichlorophenyl)-1,1-dimethylurea; DMSO, dimethyl sulfoxide; EPR, electron paramagnetic resonance; FTIR, Fourier transform infrared; OEC, oxygen evolving complex; P_{680} , primary donor of photosystem II; PSII, photosystem II; Q_A , primary plastoquinone acceptor; Q_B , secondary plastoquinone acceptor; RC, reaction center; TL, thermoluminescence; Y_Z , a redox-active tyrosine residue.

carboxylate contributions were found to occur as negative bands at 1490 and 1331 cm^{-1} and as positive bands at 1393 and 1267 cm^{-1} and to be associated only with the EPR multiline signal, not with the $g = 4.1$ signal. The 1404 cm^{-1} band which was suggested by Noguchi et al. (7) to represent the carboxylate ligand to the Mn was completely absent. With the formation of the $g = 4.1$ signal, a unique protein conformational change was suggested to occur, on the basis of analyses of the spectral features of the amide I band (1700–1600 cm^{-1}) (8–9).

With respect to the plastoquinone photoreduction, the Q_A^-/Q_A difference spectrum has been studied more extensively (5, 10–13), although exact band assignments are still under debate (14). It is thought that an infrared absorption of Q_A^- occurs at 1478 cm^{-1} , which was tentatively assigned to the $\nu(\text{CO})$ mode of Q_A^- (10). This assignment was based on the in vitro FTIR analysis of quinone redox reactions (15) and on the insensitivity of the 1478 cm^{-1} band to ^{15}N -labeling and H/D exchange (10–12). The corresponding $\nu(\text{CO})$ mode of the neutral quinone was suggested to occur at 1645 and/or 1630 cm^{-1} (10). As to infrared absorption due to Q_B^- , no information is available so far, mostly because of the difficulty in separating the Q_A signals from the Q_B signals in static FTIR measurements.

On the basis of thermoluminescence (TL) measurements, it is known that the $S_2Q_B^-$ state can be cryogenically trapped after single turnover flash excitation of dark-adapted PSII and that subsequent thermally induced charge recombination of the $S_2Q_B^-$ state gives rise to the characteristic TL band, called the B band, around 30 °C (for a review, see ref 16). From these measurements, the decay half time of $S_2Q_B^-$ was found to be in the range of 20–60 s at room temperature (17–19). The slow decay of $S_2Q_B^-$ thus allows the infrared $S_2Q_B^-/S_1Q_B$ difference spectrum to be measured by appropriate TR-FTIR spectroscopy. In this work, we report the first $S_2Q_B^-/S_1Q_B$ difference spectrum of PSII at room temperature.

MATERIALS AND METHODS

PSII-enriched membranes were prepared from hydroponically grown spinach, as described earlier (20), and stored at -80°C until used. PSII samples were suspended in SMNM medium containing 0.4 M sucrose, 40 mM Mes (pH 6.5), 10 mM NaCl, and 5 mM MgCl_2 . For the FTIR measurements, the PSII samples were centrifuged at 100 000g for 15 min to form a solid pellet. In the case where electron flow from Q_A to Q_B is to be blocked, the PSII samples were incubated in 50 mM DCMU for 10 min prior to ultracentrifugation.

The decay kinetics of the S_2 state were monitored by flash-induced O_2 polarographic measurements using a home-built Joliot-type electrode (21). A PC was used to control the data acquisition as well as to trigger a xenon flash lamp (5 ms, fwhh) used for photoexcitation. To ensure light saturation, the PSII samples were suspended at 1 mg Chl/mL. One preflash was given to the samples followed by dark-adaptation for 5 min at room temperature to enrich the S_1 state. The S_1 -enriched samples were loaded onto a platinum electrode and given one flash to generate the S_2 state. At various dark periods (denoted as t_d) after the excitation flash,

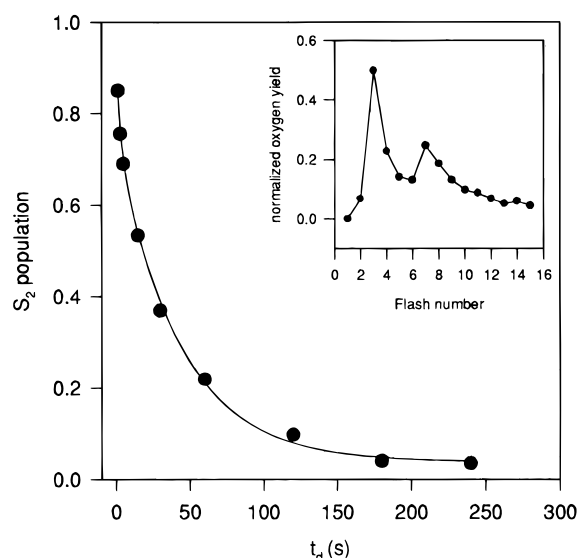


FIGURE 1: The decay of the S_2 state for PSII-enriched membranes at room temperature. PSII samples were given one flash, followed by various dark periods t_d , and a train of 15 saturating flashes (2 Hz repetitive rate). The S_2 population at various t_d was calculated by deconvolution of the O_2 yield pattern according to the Kok model (22) after normalization to the sum of the O_2 yields on flashes 2–4. Inset: a normal O_2 yield pattern after complete dark-adaptation. The steady-state O_2 -evolving activity of the PSII-enriched membranes was 600–650 $\text{mmol O}_2 (\text{mg Chl})^{-1} \text{h}^{-1}$ measured at 25 °C in the presence of 1 mM potassium ferricyanide and 50 μM phenyl-*p*-benzoquinone.

O_2 yield patterns induced by a train of 15 flashes (2 Hz repetitive rate) were measured. The S_2 population at various t_d was calculated by deconvolution of the O_2 yield pattern according to the conventional Kok model (22) using a least-squares minimization.

TR-FTIR spectra were obtained on a Bruker IFS66 spectrometer equipped with a liquid-nitrogen-cooled MCT-B detector and a KBr beam splitter as described previously (13). The spectra were recorded with a spectral resolution of 4 cm^{-1} and reproducible to $\pm 1 \text{ cm}^{-1}$ accuracy. PSII-pellet samples were deposited and sealed between two CaF_2 windows. The absorbance of the amide I band (1656 cm^{-1}) was adjusted to be ~ 0.75 au. Prior to the data acquisition, a preflash was given to the PSII sample directly in the sample chamber and dark-adapted for 5 min. After a single flash excitation, seven transient spectra averaged over 40 scans were recorded every 4.44 s. The dark spectrum was measured immediately before the flash excitation and used as the background to construct the final light-minus-dark difference spectra. The S/N ratio was improved by averaging over 80 cycles. A dark period of 5 min was used to allow the closed reaction centers to recover.

The decay of Q_A^- was determined in the same PSII sample used for FTIR measurements by monitoring the variable chlorophyll *a* fluorescence after a single excitation flash using a PAM fluorometer as described earlier (13). All measurements were performed at room temperature ($16 \pm 2^\circ\text{C}$).

RESULTS

The determination of the S_2 lifetime by O_2 polarographic measurements is presented in Figure 1. As shown in the inset, PSII-enriched membranes exhibit a damped, period-four O_2 yield pattern with peak yields occurring on the third

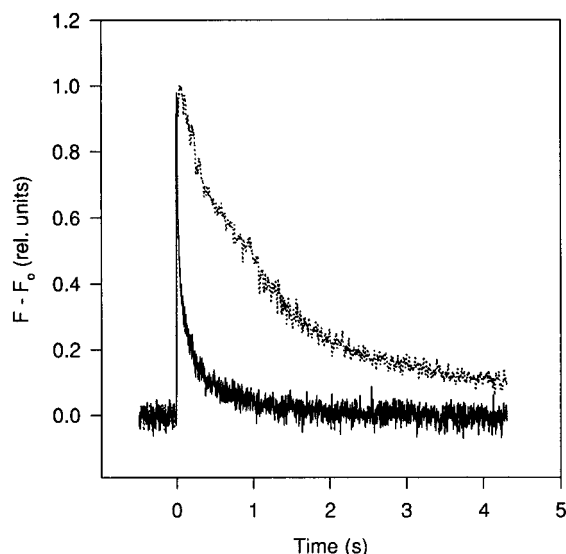


FIGURE 2: Decay of the variable chlorophyll *a* fluorescence after a single-turnover flash excitation of PSII-enriched membranes at room temperature. Solid line, no additions; dotted line, plus 50 mM DCMU. DCMU was dissolved in DMSO. The final concentration of DMSO in the PSII sample was $\sim 1\%$. Each trace is an average of five measurements.

and the seventh flashes. The O_2 yields of the first seven flashes were used to calculate the double hits and misses according to the Kok model, which were found to be 0.018 and 0.11, respectively. These parameters were then fixed for the deconvolution of the S_2 population at various t_d . A plot of the S_2 population vs t_d gives rise to the decay kinetics of the S_2 state. This is shown in the main panel of Figure 1. The decay half time for the S_2 state is estimated to be ~ 18 s under our experimental conditions, which is in approximate agreement with the half times that have been reported earlier (22–25). The half time of ~ 18 s is also close to the half time of 22 s for the back-reaction of $S_2Q_B^-$ in pea chloroplasts as determined by chlorophyll *a* fluorescence measurements (26), indicating that the deactivation of the S_2 state is mostly through charge recombination with Q_B^- under these conditions.

The electron transport on the acceptor side of PSII was also examined in the same samples as used for the FTIR measurements by monitoring the variable chlorophyll *a* fluorescence. The results are presented in Figure 2. In the absence of DCMU (solid line), the chlorophyll *a* fluorescence decays rapidly with a half time of ~ 29 ms. The fast decay of the chlorophyll *a* fluorescence is mostly attributed to the oxidation of Q_A^- by Q_B . It is known that electron transfer from Q_A^- to Q_B occurs in 100–200 μ s in chloroplasts (26–27), while in PSII-enriched membranes the forward electron transfer is slowed by a factor of at least 2 (28). Due to PSII heterogeneity, the electron transfer from Q_A^- to Q_B may not occur efficiently in a fraction of the PSII reaction centers, resulting in a slow reoxidation of Q_A^- by charge recombination with S_2 as occurs in the presence of DCMU. As also shown in Figure 2, in the presence of DCMU (dotted line), the decay of the chlorophyll *a* fluorescence is substantially slower with a half time of ~ 1 s. In this situation, a single turnover excitation of the dark-adapted PSII samples leads to the formation of $S_2Q_A^-$ only. Thus, the decay reflects mostly the charge recombination between S_2 and Q_A^- . The measured half time of ~ 1 s is in the range of the 1–3 s half

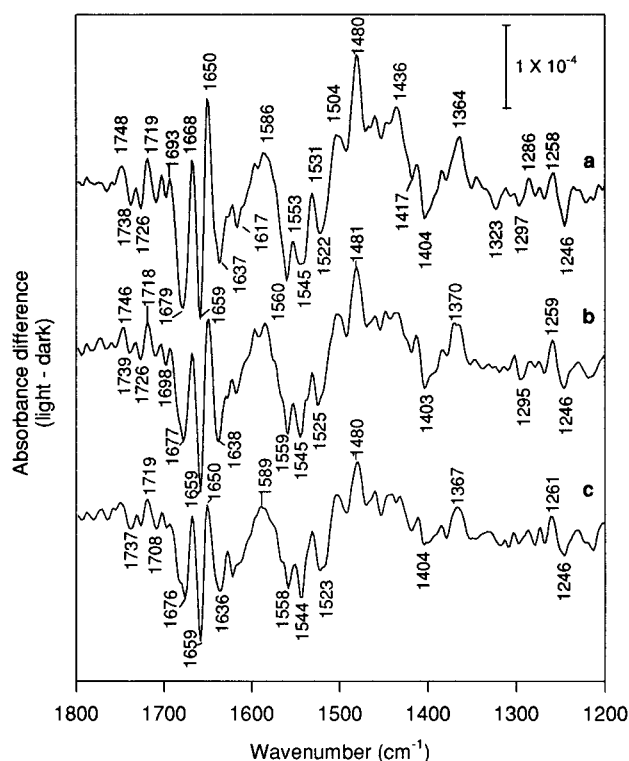


FIGURE 3: Time-dependent infrared difference spectra of PSII-enriched membranes after a single-turnover flash excitation. The spectra were measured at room temperature in the SMNM medium (pH 6.5). Traces a, b and c were measured over 4.44, 8.95, and 13.46 s after photoexcitation, respectively. Each spectrum was averaged over 3200 scans from four separate samples.

time determined for the back-reaction of $S_2Q_A^-$ from TL and variable chlorophyll *a* fluorescence measurements (for a review, see ref 16).

Figure 3 shows the time-dependent infrared difference spectra measured after a single turnover flash excitation of dark-adapted PSII-enriched membranes. As mentioned above, under these conditions, the $S_2Q_B^-$ state is formed. The light-induced $S_2Q_B^-$ should make positive contributions, whereas the S_1Q_B should make negative contributions to the difference spectra. In addition, any protein side chains and/or protein backbones perturbed upon the S_1Q_B -to- $S_2Q_B^-$ transition will also contribute to the difference spectra. As shown in Figure 3, the most intense positive band of trace a occurs at 1480 cm^{-1} . Other reproducible spectral features include positive bands at 1748, 1719, 1693, 1668, 1650, 1586, 1553, 1531, 1504, 1436, 1364, 1286, 1258 cm^{-1} and negative bands at 1738, 1726, 1679, 1659, 1637, 1617, 1560, 1545, 1522, 1417, 1404, 1323, 1297, 1246 cm^{-1} . In the subsequent traces (b and c), all bands are decaying. The intense band at 1480 cm^{-1} is of particular interest. As has been established, the $\nu(\text{CO})$ mode of Q_A^- of PSII has a contribution at 1478 cm^{-1} (10–13). It is also known that $Q_A^-Q_B$ and $Q_AQ_B^-$ states coexist in equilibrium in PSII following photoexcitation, which apparently complicates the assignment of the bands. However, the decay kinetics for the back-reaction between Q_A^- and S_2 differs from that for the back-reaction between Q_B^- and S_2 , with the former reaction being faster by a factor of ~ 18 , as shown in Figures 1 and 2. Thus, one way to identify whether the 1480 cm^{-1} band arises from Q_A^- or Q_B^- is to examine its decay kinetics. This is shown in Figure 4. As seen, the 1480 cm^{-1} band

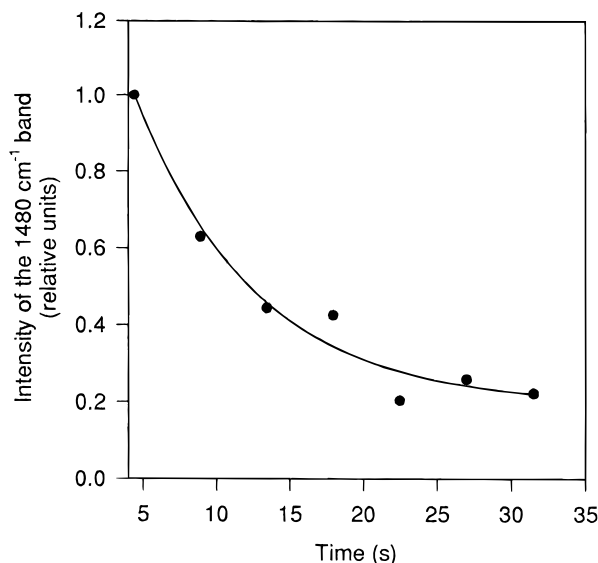


FIGURE 4: The decay of the 1480 cm^{-1} band after a single-turnover flash excitation. The signal intensity was normalized to the area under the peak height of trace a in Figure 3, having a flat baseline from 1900 to 1800 cm^{-1} where there are no infrared absorptions.

shows a slow decay in comparison with the chlorophyll *a* fluorescence decay, even in the presence of DCMU (Figure 2). More than 20% of the signal intensity remains, even in ~ 32 s after photoexcitation. The half time for the decay of the 1480 cm^{-1} band is estimated to be ~ 13 s, which is in approximate agreement with the half time of 18 s for the decay of the S_2 state as determined by oxygen polarographic measurements (Figure 1). It should be emphasized that any forms of stabilized Q_A^- do not exist after 4 s after the excitation flash in the absence of DCMU according to the data of Figure 2 (solid line), regardless of the oxidation pathway. Therefore, contributions from Q_A^- are unlikely to be present in any of the traces after trace a of Figure 3 since all of these traces were recorded on longer time scales (>4.44 s). Although we cannot completely rule out the possibility that there are some Q_A^- contributions to trace a, compared with traces b and c, trace a shows almost identical spectral features. Thus, any contributions of Q_A^- to trace a are likely to be negligible. According to Robinson and Crofts (26), the equilibrium constant between $Q_A^-Q_B$ and $Q_AQ_B^-$ is about 15–20, indicating that Q_A^- exists in only $\sim 5\%$ of the PSII RCs following photoexcitation. Thus, the presence of Q_A^- is neither thermodynamically nor kinetically favored to make significant contributions to the results shown in Figure 3.

To further check for possible Q_A contributions, we attempted to measure the $S_2Q_A^-/S_1Q_A$ difference spectrum in DCMU-treated PSII membrane samples. Presumably, a single turnover excitation of the DCMU-treated PSII membrane sample leads to the formation of the $S_2Q_A^-$ state only. Under the same measuring conditions as used for measurement of Figure 3, we could not obtain a meaningful spectrum (data not shown), indicating that the $S_2Q_A^-$ state decays more rapidly. However, the $S_2Q_A^-/S_1Q_A$ difference spectrum was obtained at a temporal resolution of 50 ms. This is shown in Figure 5. As seen, the characteristic absorptions of Q_A^-/Q_A are observed as a positive band at 1478 cm^{-1} and negative bands at 1642 and 1633 cm^{-1} . Figure 5 agrees with the $S_2Q_A^-/S_1Q_A$ difference spectrum as reported earlier (5). It

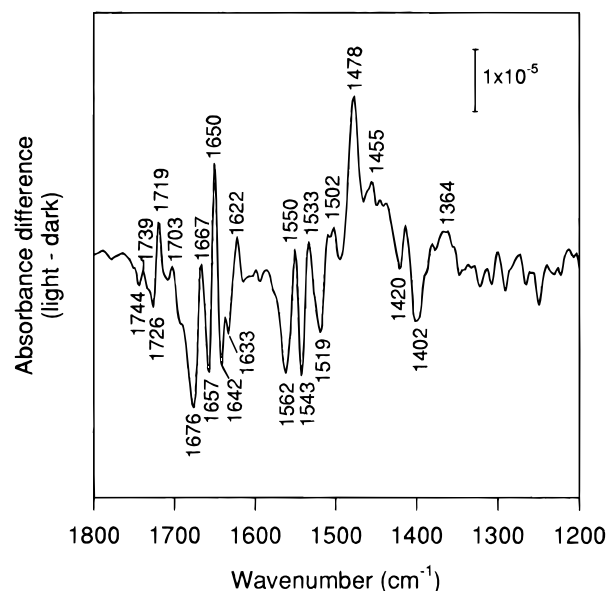


FIGURE 5: Room-temperature $S_2Q_A^-/S_1Q_A$ FTIR difference spectrum of PSII-enriched membranes after a single-turnover flash excitation. The spectrum was obtained in the presence of 50 mM DCMU in the SMNM medium (pH 6.5). The time resolution is 50 ms, and the flash frequency is 0.25 Hz. The spectrum was averaged over the first four traces of 15 experiments from four sample preparations.

is notable that the 1478 , 1642 , and 1633 cm^{-1} bands which are characteristic of Q_A^-/Q_A are not present in Figure 3.

Apart from the contributions from Q_B^-/Q_B , Figure 3 should also contain contributions from the S_2/S_1 states of the Mn cluster based on the S_2 lifetime measurement (Figure 1). In the spectral region of the amide I band, the large differential features at $1679/1668$ and $1659/1650\text{ cm}^{-1}$ are observed. A pair of bands at $1404/1364\text{ cm}^{-1}$ are also present. These features are not characteristic of the contributions from plastoquinone molecules (5, 10–13). Removal of the Mn by Tris wash abolishes these spectral features, as demonstrated in our previous work (13) as well as in (5). To facilitate comparison, trace a of Figure 3 is superimposed with the spectrum recorded in Tris-washed PSII-enriched membranes. This is shown in Figure 6. The two spectra were normalized under the most intense bands, as there is no reliable way to correct variations in Chl concentration and path length during FTIR measurements on the scale of 10^{-4} – 10^{-5} au. As shown, these two spectra are explicitly different. In the spectral region between 1800 and 1500 cm^{-1} , the large differential bands at $1679/1668$ and $1659/1650\text{ cm}^{-1}$ are not present in the Tris-washed PSII-enriched membranes. In addition, two negative bands at 1637 and 1617 cm^{-1} are also absent from the spectrum of the Tris-washed PSII-enriched membranes. In the low-frequency region (1500 – 1200 cm^{-1}), the most intense bands differ by 3 cm^{-1} . The band at 1404 cm^{-1} observed in the intact PSII-enriched membranes is lost in the Tris-washed PSII-enriched membranes. Furthermore, Figure 3 is in good agreement with the S_2/S_1 difference spectrum as reported earlier (6). A comparison is shown in Figure 7. As seen, the two spectra are strikingly similar except for an intense line at 1480 cm^{-1} in trace a.

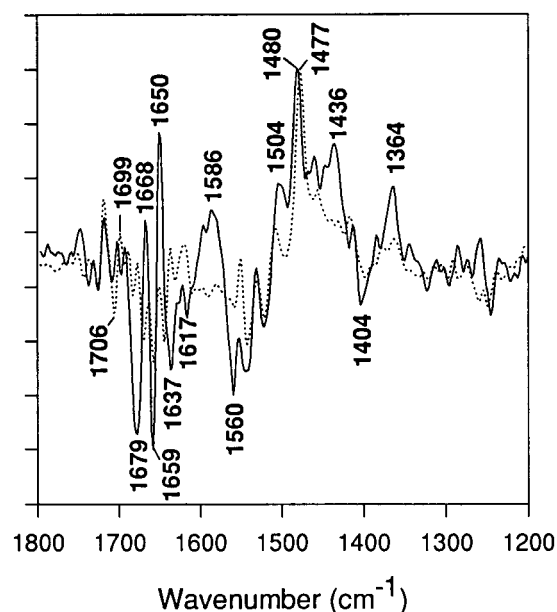


FIGURE 6: Comparison of FTIR difference spectra between intact and Tris-washed PSII-enriched membranes. Solid line, intact PSII, same as trace a of Figure 3; dotted line, Tris-washed PSII, same as trace a of Figure 6 of ref 13. The two spectra were normalized under the peak intensities at 1480 cm^{-1} for the intact PSII and 1477 cm^{-1} for the Tris-washed PSII.

DISCUSSION

In this work, we have reported the first $S_2Q_B^-/S_1Q_B$ difference spectrum of PSII measured at room temperature using TR-FTIR methods (Figure 3). An interesting feature of the spectrum is an intense positive band at 1480 cm^{-1} . Compared to the pure S_2/S_1 difference spectrum (trace b, Figure 7), this band is not present and thus is attributable to Q_B^- . However, possible contributions of Y_D and Y_Z to the data in Figure 3 are factors that may affect a correct assignment. Despite a number of investigations, band assignments regarding the vibrational modes of the two tyrosines remain controversial. As proposed (29), the $\nu(\text{CO})$ mode of Y_D^{ox} of PSII from cyanobacteria contributes at 1472 cm^{-1} . By contrast, the Y_D^{ox}/Y_D difference spectra of PSII from spinach (12) and from cyanobacteria (30) do not show any significant positive contributions around 1480 cm^{-1} . In Figure 3, there is no additional band or shoulder at 1472 cm^{-1} . Thus, it is likely that the data of Figure 3 do not contain any significant contributions from Y_D . The absence of Y_D contributions is probably due to the slow turnover of Y_D in intact PSII-enriched membranes. As reported earlier, Y_D^{ox} is stable for hours in uninhibited samples (31). In the type of PS II preparations used in this work, the decay half time of Y_D^{ox} was determined to be about 8.3 h at pH 6.5 at room temperature (32). The preflash given before the FTIR measurements shown in Figure 3 and the short time interval between photocycles (5 min) thus will keep Y_D oxidized, so that it should not contribute to the difference spectra.

Likewise, any contributions of Y_Z^{ox} from inactive centers should also be negligible in the time-resolved spectra of Figure 3. According to our previous data obtained on Mn-depleted PSII-enriched membranes (13), Y_Z^{ox} decays on the millisecond time scale ($t_{1/2} = 0.11\text{ s}$) and thus would not be detectable over the time resolution reported in Figure 3. This

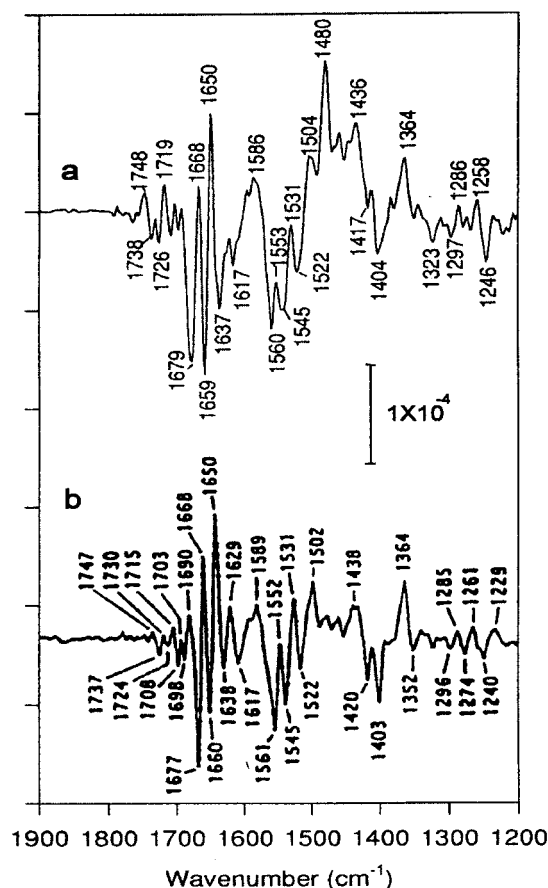


FIGURE 7: Comparison of light-minus-dark infrared difference spectra of PSII obtained after a single-turnover flash excitation at room temperature without any additions at pH 6.5 (trace a) with that obtained after continuous illumination at 250 K in the presence of 2 mM/18 mM ferri/ferrocyanide at pH 5.5 (trace b). Trace a is the same as trace a of Figure 3, while trace b is reproduced with permission from ref 7. The former represents the $S_2Q_B^-/S_1Q_B$ difference spectrum, and the latter is the pure S_2/S_1 difference spectrum.

argument is substantiated by the absence in Figure 3 of the large differential band at $1706/1699\text{ cm}^{-1}$ that has been attributed to Y_Z^{ox}/Y_Z (13). Therefore, we conclude that the 1480 cm^{-1} band arises from Q_B^- and that the time-resolved spectra in Figure 3 represent the true $S_2Q_B^-/S_1Q_B$ difference. A straightforward assignment of the 1480 cm^{-1} band is the $\nu(\text{CO})$ mode of the semiquinone anion Q_B^- in analogy to the $\nu(\text{CO})$ mode of Q_A^- which has an absorption at 1478 cm^{-1} (5, 10–13). However, without the results from isotopic labeling, this assignment should be considered tentative.

The difference in the $\nu(\text{CO})$ mode between Q_B^- and Q_A^- in PSII is 2 cm^{-1} . The infrared Q_A and Q_B signals of the bacterial RCs have been well characterized (33–37) and can be used as a comparison. In the *Rhodospseudomonas viridis* RCs, Q_A is a menaquinone and Q_B is a ubiquinone (UQ), while in the *Rb. sphaeroides* RCs, both Q_A and Q_B are UQ. In the former case Q_B^- and Q_A^- absorb at 1475 and 1478 cm^{-1} , respectively, and in the latter case Q_B^- and Q_A^- have intense absorptions at 1480 and 1467 cm^{-1} , respectively. Thus, the difference in the infrared absorptions between Q_B^- and Q_A^- among various species can vary over a large spectral range.

In PSII, both Q_A and Q_B are plastoquinone molecules. The fundamental vibrations for each should be identical, provided

that they are situated in the same chemical environment. In general, the factors that determine the C=O vibration of quinones include the nature of the chemical bond and its interactions with the surrounding environment such as hydrogen bonding, polarity, and van der Waals contact. On the basis of homology studies between the PSII and the bacterial RCs, it is known that the local environments around Q_A and Q_B are different. Q_A is situated in a more hydrophobic environment with nonpolar residues present in the Q_A pocket, eg., Leu211, Trp254, Phe262, Leu268, and Phe258. The plastoquinone ring and carbonyl oxygen may also form hydrogen bonding and/or van der Waals contact with Trp254, Thr218, His215, and Phe258 (38). According to Ruffle et al. (38), however, the amino acid residues that may be involved in forming the Q_B pocket include some polar residues, such as His215, Tyr237, Ser264, Asn266, Ser268, and His252. In particular, the hydroxyl group of Ser264 and δ -nitrogen of His215 may form hydrogen bonds with the carbonyl oxygen of Q_B . The frequency difference of the $\nu(\text{CO})$ modes of Q_B^- and Q_A^- reflects that the interactions of Q_B^- and Q_A^- with their local environments are not identical. The relatively small frequency shift (2 cm^{-1}) also indicates that the interactions are not dramatically different. However, more apparent changes may occur upon the formation of the Q_B^{2-} state or upon protonation of the Q_B molecule.

It is known that the Q_A^-/Q_A difference spectrum is characterized by the existence of an intense positive band at 1478 cm^{-1} and two negative bands around 1644 and 1632 cm^{-1} (5, 10–13). Berthomieu et al. (10) suggested that the 1644 and/or 1632 cm^{-1} bands may be due to the contributions from the $\nu(\text{CO})$ mode of the neutral quinone Q_A . It is notable that both 1644 and 1632 cm^{-1} bands observed in the $S_2Q_A^-/S_1Q_A$ and the Q_A^-/Q_A difference spectra are not present in the $S_2Q_B^-/S_1Q_B$ difference spectrum (Figure 3). As an alternative, the 1637 cm^{-1} band might reflect a contribution from the neutral quinone Q_B which overlaps with a contribution from the S_1 state. It is also possible that the $\nu(\text{CO})$ mode of the neutral Q_B does not contribute the difference spectra due to line broadening and/or asymmetry in the directions of the interacting dipole moments.

The contributions in the high-frequency region of 1750–1700 cm^{-1} are typical of free carbonyl and/or protonated carboxylate groups. The presence of positive bands at 1748 and 1719 cm^{-1} and negative bands at 1726 and 1738 cm^{-1} indicates that there may be perturbations to such carbonyl and/or carboxylate group(s). According to Figure 3, in the amide II band region, a number of negative bands are observed at 1560, 1545, and 1522 cm^{-1} and positive bands at 1553, 1531, and 1504 cm^{-1} . These bands are sensitive to ^{15}N -labeling of PSII (6). As such, these bands may originate from the amide II contributions from the polypeptide backbone and indicate protein conformational changes upon the formation of the $S_2Q_B^-$ state.

The contributions attributed to S_1 -to- S_2 transition are characterized by large differential bands in the amide I region (1700–1600 cm^{-1}) as well as a pair of bands at 1404/1364 cm^{-1} (Figure 3). It is known that the delocalized $\nu(\text{CO})$ mode of the amide I band from the polypeptide backbone contributes in the region of 1700 to 1620 cm^{-1} (39–40). In addition, the $\nu(\text{CO})$ mode of carbonyl groups from protein side chains may also contribute in this region. Thus, this

large differential feature may reflect conformational changes of the protein backbone upon the S_1 -to- S_2 transition and/or perturbations to certain Asp and/or Glu residues. The 1404/1364 cm^{-1} bands lie in the spectral range for a symmetric vibration of a COO^- group. It has been proposed that the 1404/1364 cm^{-1} bands represent the symmetric mode of a carboxylate group bridging Mn to Ca (6). In support of this assignment, the 1404/1364 cm^{-1} bands were not observed in the low-pH-treated PSII samples, where it is believed that the tightly bound Ca associated with the catalytic Mn is removed (6). Recently, the $S_2Q_A^-/S_1Q_A$ difference spectrum was studied at cryogenic temperatures in a glycerol-containing medium (8). In contrast, the 1404/1364 cm^{-1} bands were not observed upon formation of the EPR multiline signal and $g = 4.1$ signal. Rather, contributions from carboxylate groups which may ligate to the Mn cluster or be perturbed by the Mn oxidation were observed only with the formation of the multiline signal as negative bands at 1490 and 1331 cm^{-1} and positive bands at 1393 and 1267 cm^{-1} (8). Steenhuis and Barry (8) proposed that the discrepancy may arise from the low pH of 5.5, a high concentration of ferri/ferrocyanide (2 mM/18 mM), and a sucrose-containing medium used by Noguchi et al. (5–6). On the basis of our results, we exclude the first two possibilities, since the spectral features characteristic of the S_1 -to- S_2 transition are retained in Figure 3 which was measured in intact PSII membranes at pH 6.5 without any additions. As such, a possible reason for the spectral changes may be due to the different media used. Smith and Pace (41) have shown that two forms of $g = 4.1$ signals are observed in PSII with one being in a ground state and the other in an excited state of the Mn cluster, depending on illumination temperature and cryoprotectants used. In the presence of alcohol or glycerol, 200 K illumination of PSII leads to the $g = 4.1$ signal arising from an excited state, and thus the formation of the multiline signal is enhanced with the minimal formation of the $g = 4.1$ signal. In a sucrose-containing medium, however, both the multiline and $g = 4.1$ signals arise from ground states. Illumination at 200 K of PSII under this condition results in the formation of both signals. In the future, more investigations are required to clarify the glycerol effect on the infrared S_2/S_1 difference spectrum, although the preliminary data of S_2/S_1 in 30% glycerol is not in favor of such an effect (T. Noguchi, personal communication).

CONCLUSION

We have for the first time obtained the FTIR difference spectrum of $S_2Q_B^-/S_1Q_B$ of PSII at room temperature using time-resolved methods. An intense positive band is observed at 1480 cm^{-1} and is tentatively assigned to the $\nu(\text{CO})$ mode of the semiquinone anion Q_B^- . Compared to the S_2/S_1 difference spectrum obtained at 250 K (5–6), all the spectral features characteristic of the S_1 -to- S_2 transition are well preserved in the $S_2Q_B^-/S_1Q_B$ difference spectrum obtained at room temperature, indicating that the protein ligation and local environment around the Mn cluster upon the S_1 -to- S_2 transition are not significantly affected by a temperature change within 250 to 289 K.

ACKNOWLEDGMENT

We thank Drs. Marilyn Ball for use of her PAM fluorometer, Johannes Messinger for helpful discussions about

S_2 lifetime measurements, and Takumi Noguchi for valuable comments on the manuscript.

REFERENCES

1. Schelvis, J. P. M., van Noort, P. I., Anartsma, T. J., and van Gorkom, H. J. (1994) *Biochim. Biophys. Acta* 1184, 242–250.
2. Hansson, Ö., and Wydrzynski, T. (1990) *Photosynth. Res.* 23, 131–162.
3. Debus, R. J. (1992) *Biochim. Biophys. Acta* 1102, 269–352.
4. Britt, R. D. (1996) in *Oxygenic Photosynthesis* (Ort, D. R., and Yocum, C. F., Eds.) pp 137–164, Kluwer Academic Publishers, Dordrecht, The Netherlands.
5. Noguchi, T., Ono, T.-A., and Inoue, Y. (1992) *Biochemistry* 31, 5953–5956.
6. Noguchi, T., Ono, T. A., and Inoue, Y. (1995) *Biochim. Biophys. Acta* 1228, 189–200.
7. Noguchi, T., Ono, T.-A., and Inoue, Y. (1993) *Biochim. Biophys. Acta* 1143, 333–336.
8. Steenhuis, J. J., and Barry, B. A. (1997) *J. Phys. Chem. B* 101, 6652–6660.
9. Steenhuis, J. J., and Barry, B. A. (1996) *J. Am. Chem. Soc.* 118, 11927–11932.
10. Berthomieu, C., Nabadryk, E., Mänte, W., and Breton, J. (1990) *FEBS Lett.* 269, 363–367.
11. Berthomieu, C., Nabadryk, E., Breton, J., and Boussac, A. (1992) in *Research in Photosynthesis* (Murata, N., Ed.) Vol. 2, pp 53–56, Kluwer Academic Publishers, Dordrecht, The Netherlands.
12. Hienerwadel, R., Boussac, A., Breton, J., and Berthomieu, C. (1996) *Biochemistry* 35, 15447–15460.
13. Zhang, H., Razeghifard, R. M., Fischer, G., and Wydrzynski, T. (1997) *Biochemistry* 36, 11762–11768.
14. MacDonald, G. M., Steenhuis, J. J., and Barry, B. A. (1995) *J. Biol. Chem.* 270, 8420–8428.
15. Bauscher, M., Nabadryk, E., Bagley, K., Breton, J., and Mänte, W. (1990) *FEBS Lett.* 261, 191–195.
16. Vass, I., and Inoue, Y. (1992) in *The Photosystems, Structure, Function and Molecular Biology* (Barber, J., Ed.) pp 259–294, Elsevier Science Publishers B. V., Amsterdam, The Netherlands.
17. Rutherford, A. W., and Inoue, Y. (1984) *FEBS Lett.* 165, 163–170.
18. Vass, I., and Inoue, Y. (1986) *Photosynth. Res.* 10, 431–436.
19. Vass, I., Ono, T., and Inoue, Y. (1987) *Biochim. Biophys. Acta* 892, 224–236.
20. Berthold, D. A., Babcock, G. T., and Yocum, C. F. (1981) *FEBS Lett.* 134, 231–234.
21. Messinger, J., Seaton, G., Wydrzynski, T., Wacker, U., and Renger, G. (1997) *Biochemistry* 36, 6862–6873.
22. Forbush, B., Kok, B., and McGloin, M. (1971) *Photochem. Photobiol.* 14, 307–321.
23. Joliot, P., Joliot, A., Bouges, B., and Barbieri, G. (1971) *Photochem. Photobiol.* 14, 287–305.
24. Diner, B. A. (1977) *Biochim. Biophys. Acta* 460, 247–258.
25. Messinger, J. (1993) Ph.D. Thesis, Technical University Berlin, Berlin, Germany.
26. Robinson, H. H., and Crofts, A. R. (1983) *FEBS Lett.* 153, 221–226.
27. Bowes, J. M., and Crofts, A. R. (1983) *Biochim. Biophys. Acta* 590, 373–384.
28. Andréasson, L. E., Vass, I., and Styring, S. (1995) *Biochim. Biophys. Acta* 1230, 155–164.
29. MacDonald, G. M., Bixby, K. A., and Barry, B. A. (1993) *Proc. Natl. Acad. Sci. U.S.A.* 90, 11024–11028.
30. Hienerwadel, R., Boussac, A., Breton, J., Diner, B., and Berthomieu, C. (1997) *Biochemistry* 36, 14712–14723.
31. Babcock, G. T., and Sauer, K. (1973) *Biochim. Biophys. Acta* 325, 483–503.
32. Vass, I., and Styring, S. (1991) *Biochemistry* 30, 830–839.
33. Breton, J., Berthomieu, C., Thibodeau, D. L., and Nabadryk, E. (1991) *FEBS Lett.* 288, 109–113.
34. Breton, J., Thibodeau, D. L., Berthomieu, C., Mänte, W., Vermeglio, A., and Nabadryk, E. (1991) *FEBS Lett.* 278, 257–260.
35. Breton, J., Burie, J.-R., Boullais, C., Berger, G., and Nabadryk, E. (1994) *Biochemistry* 33, 12405–12415.
36. Breton, J., Boullais, C., Burie, J.-R., Nabadryk, E., and Mioskowski, C. (1994) *Biochemistry* 33, 14378–14386.
37. Breton, J., Burie, J.-R., Berthomieu, C., Berger, G., and Nabadryk, E. (1994) *Biochemistry* 33, 4953–4965.
38. Ruffle, S., Donnelly, D., Blundell, T. L., and Nugent, J. H. A. (1992) *Photosynth. Res.* 34, 287–300.
39. Susi, H., and Byler, M. D. (1983) *Biochem. Biophys. Res. Comm.* 115, 391–397.
40. Byler, D. M., and Susi, H. (1986) *Biopolymers* 25, 469–487.
41. Smith, P. J., and Pace, R. J. (1996) *Biochim. Biophys. Acta* 1275, 213–220.

BI971787H